Published in final edited form as:
Mol Microbiol. 2014 November ; 94(4): 815–827. doi:10.1111/mmi.12798.

spxA2, encoding a regulator of stress resistance in *Bacillus anthracis,* is controlled by SaiR, a new member of the Rrf2 protein family

Michiko M. Nakano[1], **Wren Kominos-Marvell**[1], **Bhagyashree Sane**[1], **Yaldah Mohammad Nader**[1], **Skye M. Barendt**[1], **Marcus B. Jones**[2], and **Peter Zuber**[1,*]

[1]Institute of Environmental Health, Oregon Health & Science University, Portland, OR 97239, USA

[2]J. Craig Venter Institute, La Jolla, CA 92037, USA

Summary

Spx, a member of the ArsC (arsenate reductase) protein family, is conserved in Gram-positive bacteria, and interacts with RNA polymerase to activate transcription in response to toxic oxidants. In *Bacillus anthracis* str. Sterne, resistance to oxidative stress requires the activity of two paralogues, SpxA1 and SpxA2. Suppressor mutations were identified in *spxA1* mutant cells that conferred resistance to hydrogen peroxide. The mutations generated null alleles of the *saiR* gene and resulted in elevated *spxA2* transcription. The *saiR* gene resides in the *spxA2* operon and encodes a member of the Rrf2 family of transcriptional repressors. Derepression of *spxA2* in a *saiR* mutant required SpxA2, indicating an autoregulatory mechanism of *spxA2* control. Reconstruction of SaiR-dependent control of *spxA2* was accomplished in *Bacillus subtilis*, where deletion analysis uncovered two *cis*-elements within the *spxA2* regulatory region that are required for repression. Mutations to one of the sequences of dyad symmetry substantially reduced SaiR binding and SaiR-dependent repression of transcription from the *spxA2* promoter *in vitro*. Previous studies have shown that *spxA2* is one of the most highly induced genes in a macrophage infected with *B. anthracis*. The work reported herein uncovered a key regulator, SaiR, of the Spx system of stress response control.

Keywords

Oxidative stress; Spx transcription regulator; Rrf2 family repressor; *Bacillus anthracis*

Introduction

Bacillus anthracis is the etiologic agent of anthrax. The most severe form of anthrax is caused by inhalation of *B. anthracis* spores. How spores are able to successfully germinate and survive the host's innate immunity to ultimately cause the deadly disease are important for further understanding of *B. anthracis* pathogenesis (Hanna & Ireland, 1999). When encountering toxic oxidants such as those produced by professional phagocytes, bacteria

*For correspondence. zuberp@ohsu.edu; Tel. (+1) 503-346 3424; Fax (+1), 503 346 3427.

upregulate the transcription of genes that function in detoxifying oxidative stressors and repairing the cellular damage that they cause (Imlay, 2008). The Spx transcription factor plays a pivotal role in combating oxidative stress in Gram-positive bacteria including *Bacillus subtilis* where investigation of Spx has been most extensively studied (Zuber, 2004). Additionally, the role of Spx in pathogenesis was uncovered in Streptococci (Chen *et al.*, 2012, Kajfasz *et al.*, 2010), which showed that paralogous Spx proteins are required for virulence. Spx, by interacting with the α subunit of RNA polymerase (RNAP) (Nakano *et al.*, 2003b, Newberry *et al.*, 2005, Lamour *et al.*, 2009), recognizes the Spx element (5′-AGCA-3′) situated around −44 of the target promoters (Nakano *et al.*, 2003a, Newberry et al., 2005, Lin *et al.*, 2013, Nakano *et al.*, 2010, Reyes & Zuber, 2008). Genes activated by the Spx-RNAP complex mostly function in alleviating oxidative stress (Nakano et al., 2003a, Rochat *et al.*, 2012) and protein aggregation induced by thiol stress (Runde et al., 2014). Oxidants such as diamide and hydrogen peroxide cause two important post-translational changes in Spx, namely, disulfide bond formation between the conserved cysteines, which is required for full Spx-dependent induction of *trxA* (thioredoxin) and *trxB* (thioredoxin reductase) transcription (Nakano *et al.*, 2005), and escape from the ClpXP-mediated proteolysis that results in an increase in Spx concentration (Nakano et al., 2003a). The regulated proteolysis of Spx in response to oxidants is mediated by the YjbH adaptor protein (Chan *et al.*, 2012, Garg *et al.*, 2009, Gohring *et al.*, 2011, Larsson *et al.*, 2007), which is a possible target of thiol stress control.

Unlike *B. subtilis* that carries a single *spxA* gene, *B. anthracis* has two Spx paralogues encoded by *spxA1* and *spxA2*. The *spxA2* gene is one of the most highly expressed *B. anthracis* genes in the infected macrophage (Bergman *et al.*, 2007). Our previous study identified distinct roles of each paralogue in cell survival during treatments with different oxidants (Barendt *et al.*, 2013). SpxA1 and SpxA2, together, confer diamide resistance, as only the double Δ*spxA1*Δ*spxA2* mutant shows sensitivity to diamide. In contrast, the Δ*spxA1* mutant, but not Δ*spxA2* mutant, is sensitive to hydrogen peroxide. Nevertheless, inducible expression of ClpXP protease-resistant SpxA1 or SpxA2 is able to restore peroxide resistance in the Δ*spxA1* mutant. This result suggests that both SpxA proteins are intrinsically capable of activating genes involved in peroxide resistance; however, either SpxA2 levels or its activity in the native form/context is not sufficient to activate genes that confer peroxide resistance. Here, we report the finding of a novel Rrf2-family transcriptional regulator, SaiR, which is conserved in the *Bacillus cereus* group and present evidence that SpxA2 is able to confer peroxide resistance in the *B. anthracis* Δ*spxA1* mutant when SaiR is absent. The study revealed a transcriptional regulatory network governed by SpxA1, SpxA2, and SaiR that operates in the control of the oxidative stress response in *B. anthracis*.

Results

The Δ*spxA1* mutant shows a conditional growth-defect phenotype

We have previously shown that the Δ*spxA1* but not Δ*spxA2* mutant is sensitive to hydrogen peroxide (Barendt et al., 2013). We show here that a null mutation in *saiR* (BAS3200) restores resistance to hydrogen peroxide in the Δ*spxA1* mutant cells. This finding arose from an unexpected observation that the Δ*spxA1* mutant (ORB8170), unlike the wild-type parent

(7702) or Δ*spxA2* mutant (ORB8438), was unable to grow on either tryptic soy broth (TSB, Neogen Co) agar or liquid media. However, the *spxA1* mutant grew well on other media such as BHI (brain heart infusion), LB (lysogeny broth), and DS (Difco sporulation) media (data not shown). Interestingly, freshly prepared TSB medium supported the growth of the Δ*spxA1* mutant, whereas TSB medium that was autoclaved and shelf-stored for more than five months (Aged TSB) did not support growth (Fig. 1A). In order to confirm that the growth defect of the Δ*spxA1* mutant on aged TSB agar was caused by the lack of SpxA1, we carried out a complementation analysis. To this end, we used a previously isolated streptomycin-resistant variant of Δ*spxA1* (ORB8398) and the Δ*spxA1* mutant carrying P*spank*(*hy*)-*spxA1* (ORB8404) (Barendt et al., 2013). ORB8404 was constructed using ICE*Bs1*-mediated conjugation (Auchtung *et al.*, 2005). The streptomycin-resistant Δ*spxA1* mutant did not grow on aged TSB agar, but the Δ*spxA1* strain expressing the inducible copy of *spxA1* grew on aged TSB (Fig. 1A). This result confirmed that the lack of SpxA1 is responsible for the observed growth defect phenotype.

Why is aged TSB medium not able to support the growth of the Δ*spxA1* mutant? One possibility is that some nutritional components might undergo decomposition during prolonged storage. As SpxA1 is a transcriptional regulator that functions as an activator under oxidative stress conditions, we wondered whether aged TSB lacked a particular amino acid that becomes limited under oxidative stress conditions. Methionine and cysteine are susceptible to oxidation and the enzyme involved in biosynthesis of branched chain amino acids is inactivated in response to reactive oxygen species (ROS) (Boehm *et al.*, 1976, Carlioz & Touati, 1986, Anjem & Imlay, 2012). Aged TSB supplemented with methionine, but not cysteine, cystine, nor a mixture of isoleucine/leucine/valine, supported growth of the Δ*spxA1* mutant.

Mutations in the *saiR* (BAS3200) gene suppress the Δ*spxA1* growth phenotype

The result that the aforementioned growth phenotype is specific to the Δ*spxA1* mutant prompted us to further investigate the phenomenon. We hoped that the investigation would provide a clue to understanding the physiological role of the two Spx paralogous proteins in oxidative stress response. We first decided to isolate suppressor mutants that grow on aged TSB medium in the absence of *spxA1*. Three independently isolated mutants (ORB8476, 8478, and 8492) were chosen to identify the compensatory mutations by using whole genome sequencing (Tufts University Core Facility Genomics). Sequence analysis of the mutant genomes in comparison with the parental Δ*spxA1* (ORB8170) genome identified SNP (single nucleotide polymorphism) and INDEL (base insertion/deletion) in BAS3200 (BA3453 according to the *B. anthracis* str. Ames nomenclature)(Table 1). The BAS3200 gene encodes a protein that belongs the Rrf2 family of transcriptional regulators. We named the BAS3200 gene *saiR* (suppressor of *spxA1*/regulator). As the mutations in *saiR* were found in the genomes of the three suppressor mutants, we determined whether all *spxA1* suppressors have *saiR* mutations. Using PCR, the *saiR* gene was amplified from the remaining *spxA1* suppressor strains and the PCR products were sequenced. As shown in Table 1, all suppressor mutants were found to carry mutations in *saiR*. These mutations include truncations and frameshifts, strongly suggesting that *saiR* loss-of-function mutations lead to the *spxA1* suppressor phenotype.

To confirm the assumption, we constructed an in-frame *saiR* deletion using a markerless allelic replacement technique developed by Janes and Stibitz (Janes & Stibitz, 2006), and introduced the Δ*saiR* mutation into the wild-type, Δ*spxA1*, and Δ*spxA1*Δ*spxA2* backgrounds. The Δ*spxA1*Δ*saiR* strain (ORB8606) restored the growth on aged TSB agar, whereas the Δ*spxA1*Δ*spxA2*Δ*saiR* strain (ORB8564) was unable to grow on the medium (Fig. 1B), indicating that the suppressor effect is indeed attributed to the lack of SaiR activity and the suppression by *saiR* requires SpxA2.

The *saiR* mutations restore hydrogen peroxide resistance in the Δ*spxA1* strain

As with the growth defect on aged TSB, the Δ*spxA1* strain is also more sensitive to hydrogen peroxide than the wild-type and Δ*spxA2* strains, as previously reported (Barendt et al., 2013). Therefore, we examined whether the *saiR* mutations also suppress the peroxide sensitivity caused by Δ*spxA1*. Both a *saiR* spontaneous suppressor (*sup6*) mutation and the in-frame deletion conferred peroxide resistance in the Δ*spxA1* strain to a similar level observed in the wild-type strain (Fig. S1). The *saiR* mutation did not increase peroxide resistance in the Δ*spxA1*Δ*spxA2* background (data not shown), which is in good agreement with the *saiR* growth phenotype on aged TSB.

The Δ*saiR* mutation results in elevated transcription of the *spxA2* operon

We investigated the genome-wide extent of *saiR* transcriptional control in *B. anthracis* to understand how *saiR* restores the growth phenotype and peroxide resistance in the Δ*spxA1* mutant. We also hoped that the study would provide insight into why SpxA2 is required for the compensatory effect of *saiR*. Microarray-based transcriptomic analysis was carried out using RNA isolated from the Δ*spxA1* and Δ*spxA1*Δ*saiR* strains. In addition, we compared the transcriptional profile between the wild-type and Δ*saiR* strains to assess the influence of SaiR on the transcriptome when SpxA1 is present. The result showed that *spxA2*, BA3455, BA3454, and BA3452 were highly upregulated in the absence of *saiR* in either the *spxA1*$^{+}$ or Δ*spxA1* background (Table 2). These four genes, together with *saiR*, likely constitute an operon and a putative ρ-independent transcription terminator is present downstream of BA3452 (Fig. 2). In addition, the microarray analysis identified that BA0787 (BAS0749) encoding a major facilitator family protein was upregulated by the *saiR* mutation and the upregulation caused by the mutation was 7-fold higher in the *spxA1* background than in the *spxA1*$^{+}$ background (Table 2). These microarray results were validated by RT-qPCR (Table 2). Based on these results, we hypothesized that SaiR represses transcription of the *spxA2* operon and the Δ*saiR* mutation results in upregulation of *spxA2*, leading to the activation of SpxA1-controlled genes, some of which are required for resistance to hydrogen peroxide and the growth on aged TSB.

One of the conserved cysteine residues is essential for SaiR repressor activity

Members of the Rrf2 family of transcription regulators such as IscR, NsrR, and CymR have a C-terminal region that serves a sensory function by interacting with effector ligands. IscR and NsrR coordinate an Fe-S cluster (Isabella *et al.*, 2009, Schwartz *et al.*, 2001, Tucker *et al.*, 2008, Yukl *et al.*, 2008, Kommineni *et al.*, 2010) and CymR forms a complex with CysK, O-acetylserine-thiol-lyase (Tanous *et al.*, 2008). The effectors often enhance DNA-

binding activity of the repressors and play pivotal roles in sensing signals such as Fe, NO, and O-acetyl serine (thus intracellular cysteine levels). The C-terminal domain of NsrR contains three conserved cysteine residues that coordinate the Fe-S cluster. The corresponding region in SaiR has two cysteines that are fully conserved in the orthologues from the *B. cereus* group (*B. anthracis*, *B. cereus*, and *Bacillus thuringiensis*), and other Bacilli including *Bacillus firmus*, *Bacillus methanolicus*, and *Geobacillus thermoglucosidasius* (Fig. S2). As posttranslational modifications of cysteine are known to play roles in redox signaling and oxidative stress response (Antelmann & Helmann, 2011), we determined whether one or both cysteines function in modulating DNA-binding activity. To test the possibility, the C89 and C96 residues were substituted with serine, and the mutant and wild-type alleles of *saiR* were introduced into the Δ*spxA1*Δ*saiR* strain (ORB8611) using ICE*Bs1* conjugation system (Auchtung et al., 2005). We examined the sensitivity of these conjugants to hydrogen peroxide in comparison with that of the wild-type, Δ*spxA1*, and Δ*spxA1*Δ*saiR* strains (Fig. 3A). The result showed that Δ*spxA1*Δ*saiR* cells producing the wild-type or C89S SaiR exhibit hydrogen peroxide sensitivity similar to the Δ*spxA1* mutant, indicating that the C89S mutation hardly affects SaiR repressor activity. In contrast, the sensitivity was comparable between the SaiR(C96S)-complementing strain and the parental Δ*spxA1*Δ*saiR* strain, which suggests that the C96S mutation leads to the loss of SaiR activity. Growth phenotype experiments on aged TSB agar also confirmed that C96 plays a more important role than C89 for SaiR transcription repressing activity (Fig. 1C).

The *spxA2* promoter carries two *cis*-acting regions required for SaiR repression of *spxA2*

The results above suggested that SaiR directly or indirectly interacts with the *spxA2* promoter and represses transcription under nonstress conditions. We examined whether the repressive effect of SaiR on *spxA2* transcription could be reconstituted in *B. subtilis*, which does not carry the *saiR* gene. A 5′-RACE experiment using RNA purified from the *B. anthracis* 7702 identified the *spxA2* transcription start site at 220 bp upstream of the translational start site. The *spxA2* fragment (−247 to +268 relative to the transcription start site) was fused to a promoter-less *lacZ* gene (Experimental procedures). The transcriptional *lacZ* fusion was integrated into the *thrC* locus, while an IPTG-inducible allele of *saiR* was placed at the *amyE* locus in *B. subtilis* 168. *spxA2* was transcribed in *B. subtilis* that lacks *saiR*, whereas transcription was highly repressed in the strain carrying *saiR* (Fig. 3B). The repression is specific to *spxA2* and *saiR*, as SaiR did not show any significant effect on transcription of *B. subtilis trxB*, a gene belonging to the Spx regulon (Nakano et al., 2003a) (data not shown). In addition, integration of the empty vector plasmid pDR111 (Britton *et al.*, 2002) into the *amyE* locus did not repress *spxA2* transcription (data not shown). The SaiR(C89S) mutant showed a 10-fold reduction in repressor activity compared to the wild-type SaiR, whereas the C96S mutation nearly abolished repression of *spxA2* transcription. Furthermore, *spxA2* transcription is fully active in the C89S C96S SaiR mutant (Fig. 3B). In order to eliminate the possibility that C96S and C89S C96S SaiR proteins are unstable in *B. subtilis*, we carried out western blot analysis. To this end, we constructed *B. subtilis* strains that produce the wild-type and the two mutant SaiR proteins tagged with 6xHis at the C-termini. To verify that the tagged SaiR is functional, we introduced *saiR-his*$_6$ at the *amyE* locus in *B. subtilis* carrying *spxA2-lacZ*. *spxA2* transcription in each strain carrying various *saiR-his*$_6$ was similar compared to the expression in the strain with the corresponding

untagged *saiR* gene (Fig. 3B). Western blot analysis of SaiR-His_6 using anti-His tag antibody showed that the C96 and C89S/C96S SaiR, like the wild-type protein, were produced in *B. subtilis* (Fig. S3). We concluded that the conserved cysteine residues, C96 in particular, play an important role in SaiR repressor activity.

In order to localize the *cis*-regulatory region of SaiR in the *spxA2* promoter, we constructed a series of promoter deletion mutations and examined the effect of SaiR on the promoter activity (Fig. 4A). The *spxA2* (−247 to +268) was used as the full-length promoter. The Δ1 (−100 to +31) promoter exhibited β-galactosidase activity similar to the full-length promoter in the absence of SaiR; however, repression by SaiR was 14-fold, much weaker than repression by the full promoter (105-fold). Three successive deletions (Δ2, Δ3, and Δ4) retained promoter activity, which was also partially repressed by SaiR, indicating that the region between −38 and +4 contains a *cis* site targeted directly or indirectly by SaiR repression (SaiR site 1). As expected from the 5′-RACE result, the Δ5 fragment (−100 to −39) was unable to promote *lacZ* expression. As SaiR represses more strongly the full-length promoter than the deleted (Δ2 to Δ4) promoters, we next determined whether the 5′ or 3′ region that is missing in the deleted promoters (from Δ1, Δ2 and Δ4) is required for full repression. The Δ6 (−100 to +268) promoter restored the full-length level repression, while the Δ7 (−247 to +31) fragment did not, demonstrating that the region downstream from +31 contains another SaiR target site (SaiR site 2). The minimum region that is fully susceptible to SaiR repression was localized between −50 and +174, as deduced from the observed expression levels of the Δ8 promoter mutant.

Members of the Rrf2-family of transcription factors are known to bind as dimers to DNA containing sequences exhibiting dyad symmetry (Shepard *et al.*, 2011). We searched for such sequences in the region between −38 and +4 where SaiR site 1 was likely residing. The sequence $ACTGTAAN_2TTtAAN_2TTACAGT$ (the lowercase t represents the centre of the symmetry) was detected in the core promoter region that overlaps with the promoter −10 element (Fig. 4B). Based on the deletion analysis, we assumed that SaiR site 2 exists between +31 and +174. A sequence of partial dyad symmetry ($ACTGTAAN_2TTtN_5TACANT$) was found in the region between +139 and +161. The sequence of the left half in SaiR site 2 shows a perfect match with the corresponding region of SaiR site 1, whereas the right half has a 5/9 match to site 1.

In order to confirm that the two *cis* sites are involved in SaiR repression, base substitutions were introduced in the putative control elements having dyad symmetry. When substitutions of two conserved bases in SaiR site 1 were introduced in the Δ2 (−50 to +31) promoter, the resultant Δ2m1 promoter was fully resistant to SaiR-dependent repression. In contrast, the m1 mutation in the Δ8 (−50 to +174, Fig. 4A) promoter that carries the two SaiR sites resulted in a partial loss of repression (see Δ8m1, Fig. 4A). Similarly, the same base substitutions in SaiR site 2 led to 35-fold repression by SaiR (see Δ8m2). In contrast, SaiR was unable to repress the Δ8m1m2 promoter, which supports the conclusion that both SaiR sites are required for full repression by SaiR. Binding of SaiR to the downstream site might function as a roadblock to RNAP elongation or in DNA loop formation together with its binding to the upstream, SaiR site 1.

SaiR directly controls *spxA2* transcription

The *in vivo spxA2* promoter analysis clearly demonstrated that SaiR repression is dependent on the core promoter (−23 to −1) region as well as the downstream but untranslated (+139 to +157) region. We next examined whether SaiR directly interacts with the dyad-symmetry motifs to repress transcription. As SaiR-His_6 was shown to be functional as described above, we overproduced the SaiR-His_6 in *E. coli* and purified as described in Experimental procedures. EMSA (electrophoretic mobility shift assay) was initially attempted to determine whether SaiR binds to the motifs identified by *in vivo* transcription study. In some cases, we obtained high-affinity binding of SaiR to the wild-type SaiR site 1 in a sequence-specific manner, but we were not always able to reproduce the results. We assumed that the SaiR-DNA complex might be easily dissociated during electrophoresis. Therefore, we conducted restriction enzyme protection assays, which do not involve gel electrophoresis of protein-DNA complex. As shown in Fig. 5A, there is a *Dra*I recognition site in the centre of SaiR site 1. If SaiR interacts with the dyad symmetry sequence, SaiR likely causes reduced accessibility of *Dra*I to the recognition site. As expected, increasing concentrations of SaiR protected the wild-type DNA from the cleavage by *Dra*I; whereas, the mutant DNA was susceptible to *Dra*I cleavage (Fig. 5B). Deleting the nucleotide at the centre resulted in the loss of *Dra*I site (Fig. 5A), thus becoming insensitive to *Dra*I (Fig. 5B), confirming that the digestion of the wild-type and mutant DNA is specific to *Dra*I. In addition, SaiR-dependent protection is not targeted directly to *Dra*I, as SaiR did not protect *Dra*I recognition sites other than the *spxA2* DNA (Fig. S4). A titration experiment indicated that 6 nM (3 nM as dimer) SaiR provides 50% protection from cleavage of the wild-type DNA (Figs. 5C and D). With the mutant DNA bearing the single base substitution that reduces symmetry, 50% inhibition of *Dra*I cleavage was observed at concentrations higher than 200 nM, but full inhibition was not attained in the range of concentrations (up to 400nM) used in the experiment. Based on these results, we concluded that SaiR binds to the sequence of dyad symmetry constituting SaiR site 1.

As the *in vivo* study showed that C96 plays an important role in SaiR repressor activity, we examined whether the C96S mutation or C89S C96S mutation results in reduced DNA binding using the *Dra*I digestion protection assay. The result showed that both mutant proteins retain DNA binding activity similar to the wild-type protein (data not shown). Based on these results, we concluded that SaiR directly binds to the SaiR sites to repress *spxA2* transcription and the C96 (or C89 and C96) residue may interact with a ligand or small protein, which was lost during purification process of SaiR.

We next determined that SaiR, by binding to the dyad symmetry, represses *spxA2* transcription *in vitro*. The linear DNA templates carry the *spxA2* promoter with and without the m1/m2 base substitutions (Δ8 and Δ8m1m2 in Fig. 4B). The template was expected to produce a 174 base run-off transcript. Addition of 16 nM SaiR resulted in reduced transcript synthesis from the wild-type promoter and transcription was almost completely repressed by 64 nM SaiR (Fig. 6). The mutant promoter is more resistant to SaiR repression, with transcript observed in reactions containing 64 nM SaiR. SaiR(C96S) was able to repress *spxA2* transcription *in vitro* to a degree similar to the wild-type protein (data now shown),

which is consistent with the result that showed no effect of C96S on DNA binding activity *in vitro*.

spxA2 transcription is upregulated in response to disulfide stress

The two conserved cysteines in SaiR are important in *spxA2* repression under nonstress conditions *in vivo*, but data from DNA binding and transcription studies *in vitro* with SaiR cysteine mutant proteins did not support the *in vivo* results. In hope of understanding how SaiR activity is regulated, we examined conditions where *spxA2* transcription is derepressed in the presence of SaiR. As SpxA2 activates genes involved in oxidative stress response and *spxA2* transcription is induced in the infected macrophage (Bergman et al., 2007), we first tested the effect of oxidizing agents that are produced in macrophages; namely, hypochlorite, hydrogen peroxide, and NO. *spxA2-lacZ* was not induced in response to NO in *B. subtilis* ORB8820 cells that produce SaiR (data not shown). RT-qPCR showed that *spxA2* transcription is induced around 8-fold in response to 0.8 or 2 mM NaOCl treatment for 10 min, whereas only 2-fold induction was detected with 1 mM hydrogen peroxide (Fig. 7A and data not shown for 0.8 mM NaOCl). ORB8820 carries *B. subtilis spx* and *spxA2* transcription is 3-fold higher in the *B. subtilis* spx^+ strain than *spx* mutant (Fig. 7B). NaOCl was known to evoke Spx-controlled disulfide stress response (Chi *et al.*, 2011). Hence, the observed *spxA2* upregulation in response to NaOCl could be due to increased activity/concentrations of *B. subtilis* Spx, the loss of SaiR activity, or both. To eliminate the ambiguity, we carried out RT-qPCR to measure the *spxA2* induction in the *spx* mutant cells in response to NaOCl. The results showed a significant decrease in the fold-induction in the absence of Spx, indicating that the induction caused by NaOCl is largely (if not solely) attributed to Spx response. Although diamide is a synthetic substance and not produced in macrophages, it is a potent thiol-oxidizing agent. As NaOCl is known to elicit disulfide stress (Chi et al., 2011, Gray *et al.*, 2013), we wondered whether diamide also increases *spxA2* transcription. When spx^+ cells were treated with 0.5 mM diamide, *spxA2* transcription was induced over 1000-fold, and more importantly, 150-fold induction was observed even in the absence of Spx. This result indicates that thiol oxidation first triggers SaiR inactivation and Spx further activates *spxA2* transcription in response to disulfide stress response.

Purified SaiR protein is not inactivated by responding to disulfide stress

RT-qPCR results showed that *spxA2* transcription is induced in *B. subtilis* that produces SaiR in response to oxidants. We examined whether SaiR directly senses diamide using the *Dra*I protection assay described earlier. Unexpectedly, incubation of SaiR with diamide, as well as with hydrogen peroxide, did not affect SaiR DNA-binding activity; in contrast, 50 μM NaOCl led to dissociation of SaiR from *spxA2* DNA carrying the SaiR box 1 (Fig. S5A). Furthermore, the single and double cysteine mutants of SaiR still responded to NaOCl (Fig. S5B). In these experiments, SaiR was treated with the oxidants at room temperature for 5 min before the addition of the *spxA2* DNA followed by *Dra*I digestion. When SaiR was incubated with the DNA before NaOCl addition, SaiR did not dissociate from *spxA2* (Fig S5C). These results suggested that diamide likely weakens the interaction between SaiR and the effector and that NaOCl does not target cysteine residues in SaiR to weaken its DNA binding activity.

Discussion

The most important finding of this study is that elevated *spxA2* transcription due to inactivation of the SaiR repressor is a prerequisite for SpxA2-dependent oxidative stress resistance. This study began with a serendipitous finding that the *spxA1* mutant is unable to grow on aged TSB but that the growth is restored by the addition of methionine. We assume that prolonged storage of the medium at room temperature might generate an oxidative condition, which leads to conversion of methionine to methionine sulfoxide (Met-SO). Although *B. anthracis* is generally a methionine auxotroph, the amount of methionine in aged TSB is sufficient to support the growth if SpxA1 is produced. An alternative but not mutually exclusive possibility is that Met-SO generated over time in TSB could be transported by the MetNPQ ABC-type transporter (Hullo *et al.*, 2004), and possibly reduced back to methionine by methionine sulfoxide reductases (Msr) in cells producing SpxA1. MsrA and MsrB catalyze the reduction of the S-epimer and the R-epimer of Met-SO, respectively [reviewed in (Ezraty *et al.*, 2005)]. The *msrAB* operon belongs to the Spx regulon in *B. subtilis* (You *et al.*, 2008). The *B. anthracis* genome contains *msrA1* and *msrA2*, the latter of which codes for bifunctional methionine sulfoxide reductase A/B protein. Our previous microarray data showed that $SpxA1^{DD}$ and $SpxA2^{DD}$ activate transcription of *msrA2* but not *msrA1*. Taken together, the *spxA1* mutant likely has a low MsrA2 activity that does not generate methionine from methionine sulfoxide, hence the *spxA1* mutant is unable to grow on aged TSB.

The *saiR* gene is located in the *spxA2* operons of *B. cereus* and *B. thuringiensis* and both SaiR-binding sites are conserved in the *spxA2* promoter of these bacteria (Fig. S6B), which strongly suggests that SaiR plays a pivotal role in the control of SpxA2-dependent transcriptional activation among the *B. cereus* group of bacteria. The *spxA2* operon genes were highly upregulated by the *saiR* mutation regardless of the presence or absence of *spxA1*. On the other hand, Δ*saiR* led to a moderate upregulation of BA0787 only in the absence of *spxA1*. We found that the BA0787 promoter contains a sequence with partial homology to the SaiR consensus binding-site (Fig. S6B). The sequence overlaps with a putative −35 sequence (or extended −10 element) and the left half-site has a 7/9 match to the consensus sequence and the right half-site showed a 4/9 match. In addition, the putative SaiR-binding sequence is also well conserved in *B. cereus* and *B. thuringiensis* (Fig. S6B), further supporting the direct role of SaiR in BA0787 transcription.

Our previous work identified genes induced by the Spx paralogues (Barendt et al., 2013). While this transcriptomic analysis was informative, it was carried out using IPTG-inducible *spx* paralogues that encode protease-resistant proteins, which likely circumvented stress-responsive transcriptional and proteolytic control. In fact, the study showed the essential role in peroxide resistance of SpxA1, but not SpxA2, in a $saiR^{+}$ background; nevertheless, protease-resistant SpxA2 restores peroxide resistance in *spxA1* mutant cells (Barendt et al., 2013). The results suggested that SpxA2 is capable of activating genes that function in peroxide resistance if the protein is present in sufficient levels. The study presented herein confirmed the assumption and uncovered SaiR-dependent *spxA2* repression, which explains the previous peroxide sensitivity results. As with *B. subtilis* Spx, SpxA2 activity is probably stimulated through disulfide-bond formation of the conserved cysteines, which could be

generated only under the conditions where SaiR-dependent *spxA2* repression is relieved either by the *saiR* mutation or a loss of SaiR activity.

The Rrf2 family transcription repressors are known to undergo modulation of DNA-binding activity in response to environmental stress (Shepard et al., 2011). Previous transcriptome studies by Hanna and co-workers showed that transcription of the putative *spxA2* operon (*spxA2*-BA3455-BA3454-*saiR*-BA3452) is activated in the last 3 h (called wave 5) of the 8 h life cycle of *B. anthracis* grown *in vitro* (Bergman *et al.*, 2006). In contrast, *spxA1* transcription was upregulated in the first 2 h (wave 1) after germination. Interestingly, the same group observed that members of the *spxA2* operon are among the most highly upregulated *B. anthracis* genes in infected macrophages (RAW264.7 cells) compared to cultures *in vitro* (Bergman et al., 2007).

Taken together, it is likely that SaiR is inactivated in macrophages. We have tested whether any oxidant produced in macrophages is able to induce *spxA2* transcription in the presence of SaiR. The results showed that NaOCl moderately induces *spxA2* among oxidants tested. A weak induction with hydrogen peroxide is in good agreement with the result of peroxide sensitivity assays indicating that *spxA1* mutant is sensitive to hydrogen peroxide unless *saiR* is mutated (compare the peroxide sensitivity between Δ*spxA1* and Δ*spxA1*Δ*saiR* in Fig. 3A). In comparison, a synthetic thiol-oxidizing reagent, diamide, induced *spxA2* to much higher levels and substantial induction was detected even in the absence of Spx. The result argues that oxidation of thiol(s) is a key to inactivation of SaiR repressor activity. However, it is unlikely that thiol oxidation of the conserved cysteines is sufficient for the loss of SaiR activity because of the following reasons. First, diamide did not affect DNA-binding activity of purified SaiR *in vitro*. Second, substitutions of the conserved cysteines did not show any effect on *in vitro* transcription nor DNA binding, despite the observation that the mutation showed a dramatic effect on *spxA2* transcription *in vivo*. We purified SaiR from *B. subtilis* as well as *E. coli*, under both aerobic and anaerobic conditions, to obtain the protein that reflects *in vivo* activity but neither approach has been successful. We currently hypothesize that a ligand/co-repressor (a metabolite or protein) that interacts with the C-terminal half of SaiR is lost during purification. Even in the absence of such a ligand, SaiR interacts with the SaiR-binding sites *in vitro*, but perhaps with lower affinity than what is achieved *in vivo* (Figs. 5 and 6), which explains why the SaiR-DNA complex was unstable during electrophoresis in EMSA experiments. In addition, SaiR lacking the ligand/co-repressor is unable to respond to the signal. In this scenario, C96 (and C89 to a lesser extent) is essential for interaction with the ligand/co-repressor that increases DNA binding activity. Diamide, by oxidizing C89/C96 or thiol(s) in the interacting partner, causes ligand/co-repressor dissociation. We are currently not certain whether the effect of NaOCl on SaiR activity *in vitro* has physiological relevance. One possibility is that once SaiR is released from the ligand, NaOCl might oxidize SaiR. If it is the case, the oxidized residue leading to target release is not cysteine, as the cysteine SaiR mutants still respond to NaOCl (Fig. S5B).

In conclusion, this study presented evidence that SaiR is a key player in the control of SpxA2-dependent transcription activation and studies are underway to identify the effector ligand/co-repressor of SaiR and the accompanying environmental/metabolic signal that controls SaiR activity.

Experimental procedures

Bacterial strains

B. anthracis strains used in this study are derivatives of the 7702 Sterne strain ($pXO1^+$ $pXO2^-$) and listed in Table S1. *B. subtilis* strains are derivatives of either JH642 or 168 as listed in Table S1. Plasmids and oligonucleotides are listed in Tables S2 and S3, respectively. A marker-less in-frame deletion of *saiR* was constructed using the method described by Janes and Stibitz (Janes & Stibitz, 2006). In constructing the *saiR* deletion, the codons specifying the first seven amino acids were fused in-frame to those for the last six amino acids.

Identification of *spxA1* suppressor mutations

Genomic DNA was isolated from the parental Δ*spxA1* (ORB8170) strain and three suppressor mutants. Sequence of genomic DNA was determined by Tufts University Core Facility Genomics. The input DNA (1μg per sample) was sheared by sonication to 200–300bp. The sheared DNA was then used as input for library preparation using TruSeq DNA Sample Preparation Kit (Illumina). The resulting fragment library was quantified and sequenced with HiSeq 2000 using SE50 format. The reads were then aligned to the reference genome, followed by SNP/Indel calling using CLC Genomics Workbench (CLC bio, Qiagen).

Transcriptomic and RT-qPCR analyses

RNA was isolated from 7702 (wild type), ORB8170 (Δ*spxA1*), ORB8571 (Δ*saiR*), and ORB8606 (Δ*spxA1*Δ*saiR*) strains grown in LB until OD_{600} reached around 0.4 to 0.5. RNA was isolated using glass beads/phenol method (Igo & Losick, 1986) and microarray analysis was carried out as described in a previous study (Barendt et al., 2013). The arrays used for hybridization contained 70-mers that were designed to hybridize to the 3′-end of transcripts. The microarray result was sorted and listed in Table S4 and the original data was deposited to NCBI GEO (accession ID: GSE57851).

RT-qPCR was performed using two independently isolated RNA samples that were used in microarray experiments and two additional RNA preparations. Normalization was conducted using *gatB* transcript, thoe level of which is largely constant during growth (Reiter *et al*., 2011), as described before (Barendt et al., 2013), and the ratio of induction was calculated with the normalized values. Oligonucleotide pairs spxA2-F3/spxA2-R3 and gatB-F1/gatB-R1 were used for *spxA2* and *gatB* RT-qPCR, respectively, and the sequences of these oligonucleotides are reported in a publication of a previous study (Barendt et al., 2013). Other oligonucleotides used for qPCR of BA0787, BA3454, and BA3455 are listed in Table S3.

Induction of *spxA2* transcription in response to oxidants was examined using *B. subtilis* spx^+ (ORB8820) and *spx* (ORB9050) strains carrying *spxA2-lacZ* and *saiR*. The *B. subtilis* strains were grown until OD_{600}=0.3–0.4, and treated with 2 mM (or 0.8 mM) NaOCl, 1 mM H_2O_2, or 0.5 mM diamide for 10 min. RNA was isolated from untreated and treated cells, and the

induction ratio was calculated after normalization with the induction ratio of the *rpoB* transcript. Oligonucleotides used for qPCR are listed in Table S3.

Complementation analysis using the wild-type, C89S-, and C96S-SaiR

SaiR complementation analysis was performed using the *B. subtilis* ICE*Bs1* system (Auchtung et al., 2005). The *saiR* gene was amplified by PCR and the resultant fragment was cloned downstream of the IPTG-inducible P*spank*(*hy*) promoter in pDR111 (Britton et al., 2002) to generate pSS9. The fragment containing P*spank*(*hy*)-*saiR* and the *lacI* gene was isolated from pSS9 and subcloned into pJMA402, an ICE*Bs1* conjugation system vector plasmid, resulting in pMMN850. The cysteine substitution mutations were generated using two-step site-directed PCR mutagenesis and a similar procedure used for the pMMN850 construction was applied to generate pMMN851(C89S) and pMMN852(C96S). Introduction of the wild-type and mutant *saiR* alleles into the *B. anthracis* genome was carried out by mating streptomycin-resistant *B. anthracis* with *B. subtilis* strains carrying the *saiR* genes in recombinant ICE*Bs1*.

Determination of the *spxA2* transcription start site

RNA was purified as described above from the 7702 parental strain and 5′-RACE was carried out using 5′-RACE system (Invitrogen) per manufacture's instructions.

The *spxA2* promoter analysis

Repression of *spxA2* transcription by SaiR was reconstituted in a heterologous system using *B. subtilis* 168. Various regions of the *spxA2* promoter were amplified by PCR and cloned into a promoter-probe vector, pDG793 (Guérout-Fleury *et al.*, 1996) to generate transcriptional *lacZ* fusions. The resulting plasmids were used to transform *B. subtilis* 168, which leads to the integration of the *lacZ* fusions into the *thrC* locus. Base substitutions of the *spxA2* promoter were performed using PCR-based site-directed mutagenesis and the mutated promoters were cloned in pDG793. The wild-type *saiR* gene amplified from 7702 genomic DNA was cloned in pDR111 that carries an IPTG-inducible promoter. The mutant alleles of *saiR*, which bear substitutions of Cys89, Cys96, and Cys89/96 with serine, were generated by site-directed mutagenesis and cloned in pDR111. These plasmids were used to transform *B. subtilis* to generate the strains carrying the wild-type and mutant *saiR* genes at the *amyE* locus. Although a promoter-less *saiR* was placed downstream of the IPTG-inducible P*spank*(*hy*) promoter, repression was observed even in the absence of IPTG due to the leaky IPTG-inducible promoter. Hence, all experiments using P*spank*(*hy*)-*saiR* in this study were carried out without IPTG, except otherwise stated.

Purification of SaiR protein

SaiR carrying a C-terminal 6xhistidine tag (SaiR-His_6) was produced and purified from *E. coli*. The *saiR* gene was amplified from pMMN850 and the PCR product was cloned in pET23a to generate pMMN856. To produce SaiR(C89S) and SaiR(C96S), pMMN857 and pMMN858 were constructed similarly using pMMN851 and pMMN852 as templates, respectively. The *saiR* gene with the C89S C96S mutation was generated by two-step PCR-based site-directed mutagenesis using pSS10 as template and cloned into pET23a to

construct pMMN881. *E. coli* BL21(DE3)pLysS carrying each plasmid was used to overproduce SaiR-His_6 and mutant derivatives. Purification was carried out using Ni-NTA resin (Thermo Scientific) according to manufacturer's protocol. To determine whether SaiR-His_6 is functional, *saiRhis*$_6$ was amplified using pMMN856, pMMN858, and pMMN881 as template and the resultant fragment was cloned in pDR111 to generate *amyE*-integration plasmids, pMMN880, pYA1, and pYA3, respectively. SaiR repressor activity was tested using the full-length *spxA2-lacZ*, as described above.

Restriction enzyme protection assay

DNA carrying the wild-type SaiR site 1 was generated by annealing complementary oligonucleotides oMN14-666 and oMN14-667. The resultant double stranded DNA corresponds to the region between −28 and +5 in the *spxA2* promoter. Similarly, DNA carrying the base substitution (C-22T) or deletion of −12T was generated by annealing of oMN14-668/oMN14-669 and oMN14-670/oMN14-671, respectively. The sequences of these oligonucleotides are listed in Table S3. One of the oligonucleotides (oMN14-666, oMN14-668, or oMN14-669) labeled with T4 polynucleotide kinase and γ-^{32}P ATP was annealed with the unlabeled complementary oligonucleotide. Unincorporated γ-^{32}P ATP was removed by nucleotide removal kit (Qiagen). The labeled DNA was mixed with various concentrations of SaiR-His_6 in 9 μl of 1x CutSmart buffer (50 mM potassium acetate, 20 mM Tris-acetate, 10 mM magnesium acetate, 100 μg ml^{-1} BSA, pH 7.9: New England BioLabs) and the mixture was incubated at room temperature for 20 min. After the addition of 1 μl of freshly diluted *Dra*I (0.2 units), digestion was carried out at room temperature for 30 min before heat inactivation at 65°C for 20 min. DNA was resolved on a pre-run 15% native polyacrylamide gel in TAE buffer.

In vitro transcription

In vitro transcription was carried out using the wild-type and mutant *spxA2* promoter fragments. The wild-type template was PCR amplified from pMMN874 using 793up and oMN13-638 and the mutant template was generated using 793up and oMMN14-661 with pMMN879 as template. The wild-type and mutant templates were identical with Δ8 and Δ8 m1m2 (in Fig. 4A), respectively, except that an extra 79 bp originating from pDG793 was adjacent to −50 of *spxA2*. The expected transcript size was 174 bases. A reaction mixture (20 μl total) contained 40 mM Tris-HCl (pH 8.0), 10 mM $MgCl_2$, 5% glycerol, 0.1 mM EDTA, 1 mM DTT, 0.1 mg ml^{-1} bovine serum albumin, 10 nM template DNA, 25 nM RNAP, and increasing concentrations of SaiR. *B. subtilis* His-tagged RNAP and σ^A protein previously purified (Lin et al., 2013) were preincubated on ice for 30 min (the final concentration used was 25 nM and 125 nM, respectively). The reaction mixture was incubated at 37°C for 10 min, and transcription was started by the addition of GTP, CTP, ATP (20 μM each), UTP (1 μM), and 5 μCi of α-^{32}P UTP. The reaction was stopped after 10 min, precipitated with ethanol, and products were resolved on a pre-run 6% polyacrylamide-urea gel. Sequence ladders were generated using Thermo Sequenase Cycle Sequencing Kit (Affimetrix) with the labeled downstream oligonucleotide (oMN13-638) and pMMN874.

Supplementary Material

Refer to Web version on PubMed Central for supplementary material.

Acknowledgments

This work is supported by National Institutes of Health Grants AI092313 and GM045898 (to P.Z.) and in part by National Science Foundation Grant MCB1157424 (to M.M.N.). S.M.B. is supported in part by NIH 5T32AI007472 and Y.M.N. was supported Equity Summer Internship Program by Center for Diversity & Inclusion at OHSU. We thank Dr. Boris Belitsky for helpful technical advice.

References

Anjem A, Imlay JA. Mononuclear iron enzymes are primary targets of hydrogen peroxide stress. J Biol Chem. 2012; 287:15544–15556. [PubMed: 22411989]

Antelmann H, Helmann JD. Thiol-based redox switches and gene regulation. Antioxidants & redox signaling. 2011; 14:1049–1063. [PubMed: 20626317]

Auchtung JM, Lee CA, Monson RE, Lehman AP, Grossman AD. Regulation of a *Bacillus subtilis* mobile genetic element by intercellular signaling and the global DNA damage response. Proc Natl Acad Sci USA. 2005; 102:12554–12559. [PubMed: 16105942]

Barendt S, Lee H, Birch C, Nakano MM, Jones M, Zuber P. Transcriptomic and phenotypic analysis of paralogous spx gene function in *Bacillus anthracis* Sterne. Microbiology Open. 2013; 2:695–714. [PubMed: 23873705]

Bergman NH, Anderson EC, Swenson EE, Janes BK, Fisher N, Niemeyer MM, et al. Transcriptional profiling of *Bacillus anthracis* during infection of host macrophages. Infect Immun. 2007; 75:3434–3444. [PubMed: 17470545]

Bergman NH, Anderson EC, Swenson EE, Niemeyer MM, Miyoshi AD, Hanna PC. Transcriptional profiling of the *Bacillus anthracis* life cycle in vitro and an implied model for regulation of spore formation. J Bacteriol. 2006; 188:6092–6100. [PubMed: 16923876]

Boehm DE, Vincent K, Brown OR. Oxygen and toxicity inhibition of amino acid biosynthesis. Nature. 1976; 262:418–420. [PubMed: 785275]

Britton RA, Eichenberger P, Gonzalez-Pastor JE, Fawcett P, Monson R, Losick R, Grossman AD. Genome-wide analysis of the stationary-phase sigma factor (sigma-H) regulon of *Bacillus subtilis*. J Bacteriol. 2002; 184:4881–4890. [PubMed: 12169614]

Carlioz A, Touati D. Isolation of superoxide dismutase mutants in Escherichia coli: is superoxide dismutase necessary for aerobic life? EMBO J. 1986; 5:623–630. [PubMed: 3011417]

Chan CM, Garg S, Lin AA, Zuber P. *Geobacillus thermodenitrificans* YjbH recognizes the C-terminal end of *Bacillus subtilis* Spx to accelerate Spx proteolysis by ClpXP. Microbiology. 2012; 158:1268–1278. [PubMed: 22343351]

Chen L, Ge X, Wang X, Patel JR, Xu P. SpxA1 involved in hydrogen peroxide production, stress tolerance and endocarditis virulence in *Streptococcus sanguinis*. PLoS One. 2012; 7:e40034. [PubMed: 22768210]

Chi BK, Gronau K, Mader U, Hessling B, Becher D, Antelmann H. S-bacillithiolation protects against hypochlorite stress in *Bacillus subtilis* as revealed by transcriptomics and redox proteomics. Mol Cell Proteomics. 2011; 10 M111 009506.

Ezraty B, Aussel L, Barras F. Methionine sulfoxide reductases in prokaryotes. Biochim Biophys Acta. 2005; 1703:221–229. [PubMed: 15680230]

Garg SK, Kommineni S, Henslee L, Zhang Y, Zuber P. The YjbH protein of *Bacillus subtilis* enhances ClpXP-catalyzed proteolysis of Spx. J Bacteriol. 2009; 191:1268–1277. [PubMed: 19074380]

Gohring N, Fedtke I, Xia G, Jorge AM, Pinho MG, Bertsche U, Peschel A. New role of the disulfide stress effector YjbH in beta-lactam susceptibility of *Staphylococcus aureus*. Antimicrob Agents Chemother. 2011; 55:5452–5458. [PubMed: 21947404]

Gray MJ, Wholey WY, Jakob U. Bacterial responses to reactive chlorine species. Annu, Rev, Microbiol. 2013; 67:141–160. [PubMed: 23768204]

Guérout-Fleury AM, Frandsen N, Stragier P. Plasmids for ectopic integration in *Bacillus subtilis*. Gene. 1996; 180:57–61. [PubMed: 8973347]

Hanna PC, Ireland JA. Understanding *Bacillus anthracis* pathogenesis. Trends Microbiol. 1999; 7:180–182. [PubMed: 10383221]

Hullo MF, Auger S, Dassa E, Danchin A, Martin-Verstraete I. The *metNPQ* operon of *Bacillus subtilis* encodes an ABC permease transporting methionine sulfoxide, D- and L-methionine. Res Microbiol. 2004; 155:80–86. [PubMed: 14990259]

Igo MM, Losick R. Regulation of a promoter that is utilized by minor forms of RNA polymerase holoenzyme in *Bacillus subtilis*. J Mol Biol. 1986; 191:615–624. [PubMed: 3100810]

Imlay JA. Cellular defenses against superoxide and hydrogen peroxide. Annu Rev Biochem. 2008; 77:755–776. [PubMed: 18173371]

Isabella VM, Lapek JD Jr, Kennedy EM, Clark VL. Functional analysis of NsrR, a nitric oxide-sensing Rrf2 repressor in *Neisseria gonorrhoeae*. Mol Microbiol. 2009; 71:227–239. [PubMed: 19007408]

Janes BK, Stibitz S. Routine markerless gene replacement in *Bacillus anthracis*. Infect Immun. 2006; 74:1949–1953. [PubMed: 16495572]

Kajfasz JK, Rivera-Ramos I, Abranches J, Martinez AR, Rosalen PL, Derr AM, et al. Two Spx proteins modulate stress tolerance, survival, and virulence in *Streptococcus mutans*. J Bacteriol. 2010; 192:2546–2556. [PubMed: 20233935]

Kommineni S, Yukl E, Hayashi T, Delepine J, Geng H, Moënne-Loccoz P, Nakano MM. Nitric oxide-sensitive and -insensitive interaction of *Bacillus subtilis* NsrR with a ResDE-controlled promoter. Mol Microbiol. 2010; 78:1280–1293. [PubMed: 21091510]

Lamour V, Westblade LF, Campbell EA, Darst SA. Crystal structure of the in vivo-assembled *Bacillus subtilis* Spx/RNA polymerase alpha subunit C-terminal domain complex. J Struct Biol. 2009; 168:352–356. [PubMed: 19580872]

Larsson JT, Rogstam A, von Wachenfeldt C. YjbH is a novel negative effector of the disulphide stress regulator, Spx, in *Bacillus subtilis*. Mol Microbiol. 2007; 66:669–684. [PubMed: 17908206]

Lin AA, Walthers D, Zuber P. Residue substitutions near the redox center of *Bacillus subtilis* Spx affect RNA polymerase interaction, redox control and Spx-DNA contact at a conserved cis-acting element. J Bacteriol. 2013; 195:3967–3978. [PubMed: 23813734]

Nakano MM, Lin A, Zuber CS, Newberry KJ, Brennan RG, Zuber P. Promoter recognition by a complex of Spx and the C-terminal domain of the RNA polymerase alpha subunit. PLoS One. 2010; 5:e8664. [PubMed: 20084284]

Nakano S, Erwin KN, Ralle M, Zuber P. Redox-sensitive transcriptional control by thiol/disulphide switch in the global regulator, Spx. Mol Microbiol. 2005; 55:498–510. [PubMed: 15659166]

Nakano S, Kuster-Schock E, Grossman AD, Zuber P. Spx-dependent global transcriptional control is induced by thiol-specific oxidative stress in *Bacillus subtilis*. Proc Natl Acad Sci USA. 2003a; 100:13603–13608. [PubMed: 14597697]

Nakano S, Nakano MM, Zhang Y, Leelakriangsak M, Zuber P. A regulatory protein that interferes with activator-stimulated transcription in bacteria. Proc Natl Acad Sci USA. 2003b; 100:4233–4238. [PubMed: 12642660]

Newberry KJ, Nakano S, Zuber P, Brennan RG. Crystal structure of the *Bacillus subtilis* anti-alpha, global transcriptional regulator, Spx, in complex with the alpha C-terminal domain of RNA polymerase. Proc Natl Acad Sci USA. 2005; 102:15839–15844. [PubMed: 16249335]

Reiter L, Kolsto AB, Piehler AP. Reference genes for quantitative, reverse-transcription PCR in *Bacillus cereus* group strains throughout the bacterial life cycle. J Microbiol Methods. 2011; 86:210–217. [PubMed: 21620905]

Reyes DY, Zuber P. Activation of transcription initiation by Spx: formation of transcription complex and identification of a cis-acting element required for transcriptional activation. Mol Microbiol. 2008; 69:765–779. [PubMed: 18687074]

Rochat T, Nicolas P, Delumeau O, Rabatinova A, Korelusova J, Leduc A, et al. Genome-wide identification of genes directly regulated by the pleiotropic transcription factor Spx in *Bacillus subtilis*. Nucleic Acids Res. 2012; 40:9571–9583. [PubMed: 22904090]

Schwartz CJ, Giel JL, Patschkowski T, Luther C, Ruzicka FJ, Beinert H, Kiley PJ. IscR, an Fe-S cluster-containing transcription factor, represses expression of *Escherichia coli* genes encoding

Fe-S cluster assembly proteins. Proc Natl Acad Sci USA. 2001; 98:14895–14900. [PubMed: 11742080]

Shepard W, Soutourina O, Courtois E, England P, Haouz A, Martin-Verstraete I. Insights into the Rrf2 repressor family--the structure of CymR, the global cysteine regulator of *Bacillus subtilis*. The FEBS journal. 2011; 278:2689–2701. [PubMed: 21624051]

Tanous C, Soutourina O, Raynal B, Hullo MF, Mervelet P, Gilles AM, et al. The CymR regulator in complex with the enzyme CysK controls cysteine metabolism in *Bacillus subtilis*. J Biol Chem. 2008; 283:35551–35560. [PubMed: 18974048]

Tucker NP, Hicks MG, Clarke TA, Crack JC, Chandra G, Le Brun NE, et al. The transcriptional repressor protein NsrR senses nitric oxide directly via a [2Fe-2S] cluster. PLoS ONE. 2008; 3:e3623. [PubMed: 18989365]

You C, Sekowska A, Francetic O, Martin-Verstraete I, Wang Y, Danchin A. Spx mediates oxidative stress regulation of the methionine sulfoxide reductases operon in *Bacillus subtilis*. BMC Microbiol. 2008; 8:128. [PubMed: 18662407]

Yukl ET, Elbaz MA, Nakano MM, Moënne-Loccoz P. Transcription factor NsrR from *Bacillus subtilis* senses nitric oxide with a 4Fe-4S cluster. Biochemistry. 2008; 47:13084–13092. [PubMed: 19006327]

Zuber P. Spx-RNA polymerase interaction and global transcriptional control during oxidative stress. J Bacteriol. 2004; 186:1911–1918. [PubMed: 15028674]

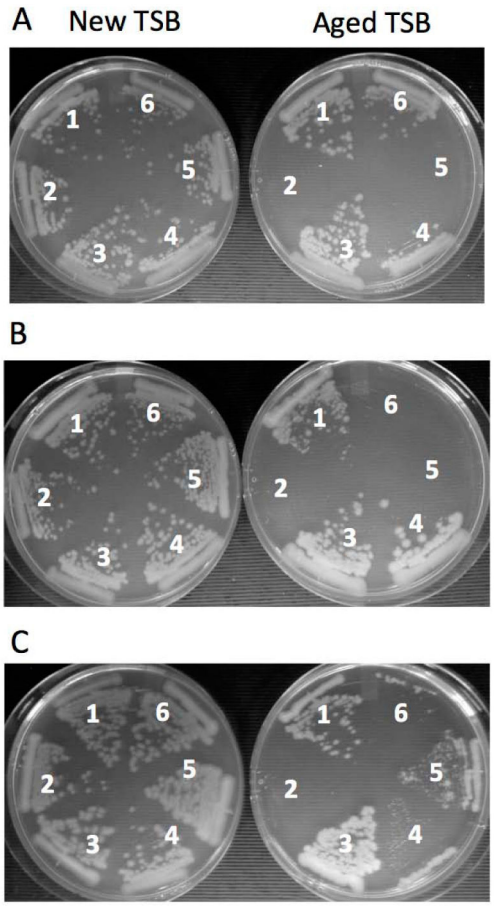

Fig. 1. Growth phenotype of *Bacillus anthracis* 7702 and its mutant derivatives on fresh and aged TSB agar media

A. The Δ*spxA1* strain is unable to grow on aged TSB unlike the wild-type parent and the Δ*spxA2* mutant. Strains: 1, wt (7702 Sterne); 2, Δ*spxA1* (ORB8170); 3, Δ*spxA2* (ORB8438); 4, wtStr^r (7702 SR1); 5, Δ*spxA1*Str^r (ORB8398); 6, Δ*spxA1*Str^r+*spxA1*^{DD} (ORB8404).

B. The *saiR* mutations restore the growth of the Δ*spxA1* mutant on aged TSB agar, but not of the Δ*spxA1*Δ*spxA2* mutant. Strains: 1, wt (7702 Sterne); 2, Δ*spxA1* (ORB8170); 3, Δ*spxA1sup6* (ORB8492); 4, Δ*spxA1*Δ*saiR* (ORB8606); 5, Δ*spxA1*Δ*spxA2* (ORB8285); Δ*spxA1*Δ*spxA2*Δ*saiR* (ORB8564).

C. The substitution of C96 in SaiR leads to a loss of repressor activity. Strains: 1, wt (7702 Sterne); 2, Δ*spxA1* (ORB8170); 3, Δ*spxA1*Δ*saiR* (ORB8606); 4, Δ*spxA1*Δ*saiR*+*saiR*(C89S) (ORB8723); 5, Δ*spxA1*Δ*saiR*+*saiR*(C96S) (ORB8724); 6, Δ*spxA1*Δ*saiR*+*saiR*(wt) (ORB8725).

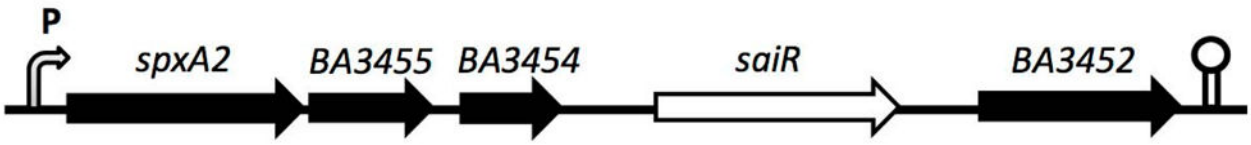

Fig. 2.

spxA2 and *saiR* reside within a five-gene operon in *B. anthracis*. *spxA2* and *saiR* are likely transcribed from the *spxA2* promoter together with three other genes shown using Ames nomenclature. The function of these three genes is unknown. The bent arrow marked with P indicates the operon promoter and the direction of transcription, and the lollipop indicates a putative ρ-independent transcription terminator.

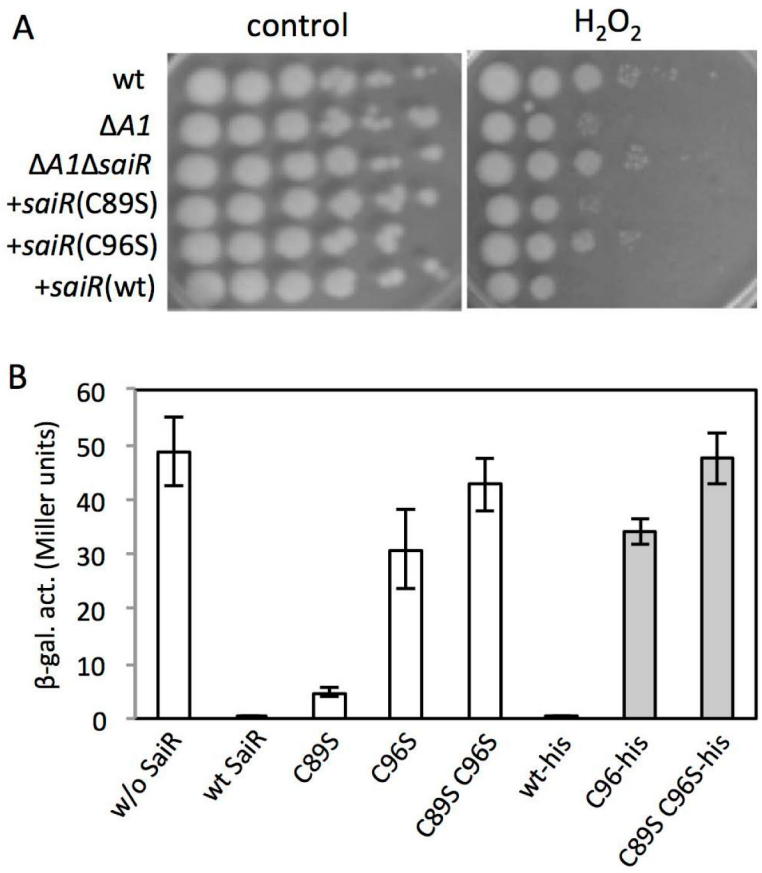

Fig. 3. Cys96 in SaiR is required for repressor activity

A. H_2O_2 sensitivity assays were carried out as previously described. Five μl of 10-fold serial dilutions of cells (left to right) were spotted onto LB agar with and without 0.44 mM H_2O_2. The *saiR* genes, which encode the wild-type, C89S, and C96S protein, were introduced into the ICE*Bs1* element of the Δ*spxA1*Δ*saiR* mutant. Strains: wt (7702SR1); Δ*spxA1* (ORB8398); Δ*spxA1*Δ*saiR* (ORB8611); Δ*spxA1*Δ*saiR* +*saiR*(wt) (ORB8725); Δ*spxA1*Δ*saiR* +*saiR*(C89S) (ORB8723); Δ*spxA1*Δ*saiR* +*saiR*(C96S) (ORB8724).

B. SaiR represses *spxA2* transcription in *B. subtilis*. Open bars show *spxA2-lacZ* expression in the absence of SaiR (ORB8884), in the presence of wild-type SaiR (ORB8820), SaiR(C89S) (ORB8825), SaiR(C96S) (ORB8826), and SaiR(C89S C96S) (ORB9055). The *spxA2* promoter contains the region between −247 and +268 relative to the *spxA2* transcription start site. Gray bars show that the his_6 tag has no effect on the activity of SaiR. Strains: wild-type *saiR*-his_6 (ORB8985); *saiR*(C96S)-his_6 (ORB9047); *saiR*(C89S C96S)-his_6 (ORB9064).

A

Deletion and mutation analysis of *spxA2* promoter

P*spxA2*	location		β-gal. act. (Miller units)		fold
Name	up	down	-SaiR	+SaiR	repression
full	-247	+268	41.1±6.7	0.39±0.12	105x
Δ1	-100	+31	53.8±3.8	3.8±0.65	14x
Δ2	-50	+31	52.9±11.8	2.1±0.16	25x
Δ3	-50	+4	40.3±3.4	3.0±0.41	13x
Δ4	-38	+31	28.3±2.9	1.0±0.13	28x
Δ5	-100	-39	0.26±0.06	0.30±0.04	0.9x
Δ6	-100	+268	31.1±2.7	0.27±0.07	115x
Δ7	-247	+31	33.7±4.1	3.7±0.16	9x
Δ8	-50	+174	27.3±6.6	0.16±0.09	171x
Δ2m1	-50	+31	56.0±8.0	51.2±6.4	1.1x
Δ8m1	-50	+174	34.7±3.7	1.1±0.11	32x
Δ8m2	-50	+174	34.5±6.9	0.98±0.07	35x
Δ8m1m2	-50	+17	24.4±0.78	28.3±2.4	0.9x

B

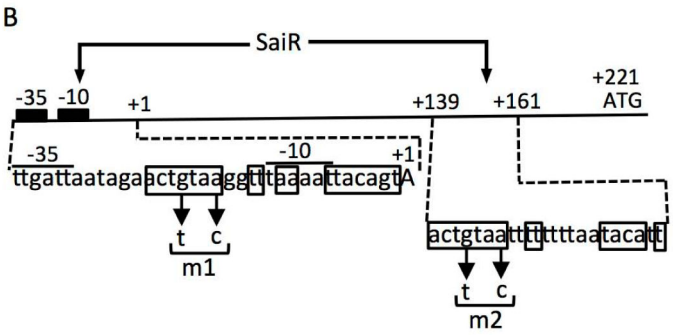

Fig. 4. The *spxA2* promoter contains two *cis*-sites required for SaiR repression

A. Deletion and mutational analysis of the *spxA2* promoter. Endpoints of the promoter fused to *lacZ* are shown in numbers relative to the transcriptional start site. Each strain was grown in LB and cells were harvested around $OD_{600}\approx0.4$ to measure β-galactosidase activities. Experiments were repeated at least three times using independent isolates obtained from strain construction and the averages are shown with standard deviations.

B. A schematic map of the *spxA2* promoter region. The location of the transcription site, the core promoter, and the translation start site are marked as +1, −10 and −35, and ATG, respectively. The nucleotide sequences of the two SaiR sites are shown below the map. Boxed nucleotides constitute a dyad symmetry sequence in site 1 and a partial dyad symmetry sequence in site 2. Arrows show the base substitutions introduced in site 1 (m1) and site 2 (m2).

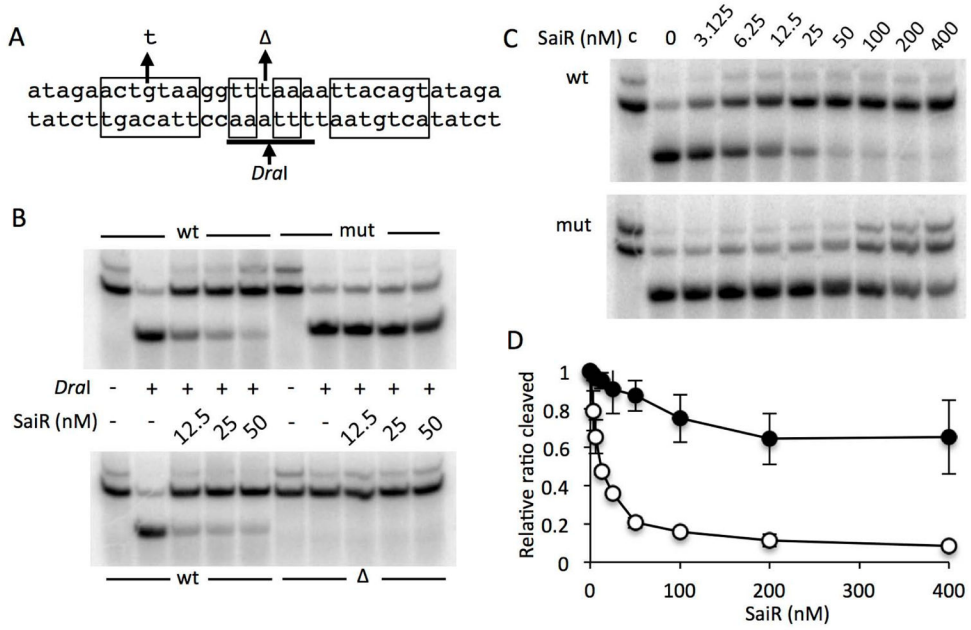

Fig. 5. SaiR directly interacts with the *spxA2* core promoter

A. The probes used for *Dra*I-digestion protection assay. The sequence from −28 to +5 (relative to the transcriptional start site) of the *spxA2* promoter is shown. The nucleotide sequences in rectangular boxes indicate the dyad symmetry required for SaiR repression. The arrows above the sequence show a base substitution and deletion used in the protection assay. The *Dra*I recognition sequence is underlined and digestion site is marked by the arrow below the sequence.

B. The wild-type probe and the probe carrying the base substitution (mut) and deletion (Δ) were incubated without or with various concentrations of SaiR-His_6, followed by *Dra*I digestion. The results are representative of four independent experiments.

C. Titration of SaiR for protection against *Dra*I digestion. All lanes except those marked with c were from reactions treated with *Dra*I as described in Experimental procedures.

D. Results in triplicate of reactions shown in Fig. 5C were used to quantify band intensities using Image J. First, intensity of digested band in each lane was divided by the sum of digested and undigested band intensities in the corresponding lane (ratio cleaved). The relative ratio cleaved was calculated by dividing the ratio cleaved in each lane by the ratio obtained from the lane without SaiR. Symbols: open circles, the wild-type probe; closed circles, the probe with the base substitution.

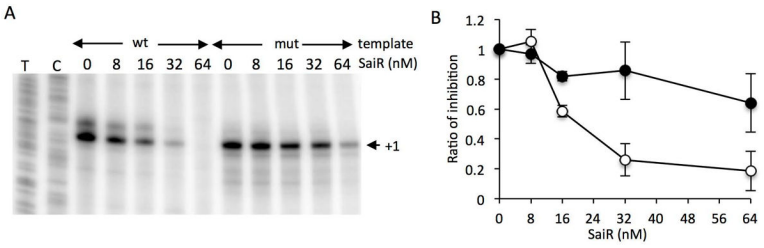

Fig. 6. SaiR represses *spxA2* transcription *in vitro*

A. The wild-type and mutant (m1m2) templates were incubated with 25 nM RNAP at 37 C for 10 min with increasing concentrations of SaiR-His_6. Transcription was initiated by the addition of nucleotide mixtures including radioactive UTP as described in Experimental procedures. T and C sequencing ladders are also shown. The results are representative of three independent experiments.

B. The intensity of the corresponding bands was quantified with ImageJ and is shown as the ratio of transcript level in the presence and absence of SaiR for each template. The values are averages of three independent experiments with standard deviations. Symbols: open circles, the wild-type template; closed circles, the mutant template.

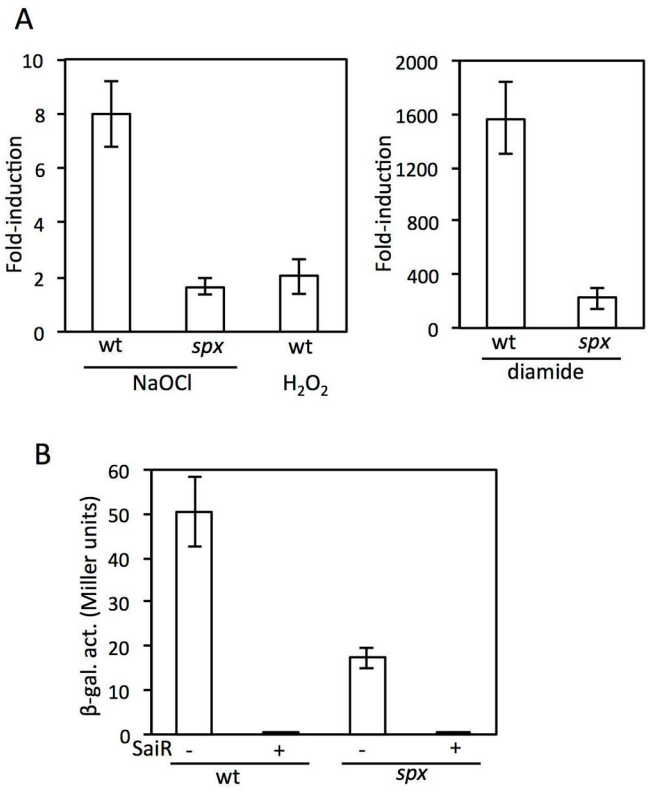

Fig. 7. Transcription of *spxA2* is upregulated by *B. subtilis* Spx *in vivo* in the absence of SaiR and transcription is induced in response to oxidants in the presence of SaiR

A. RT-qPCR of *spxA2* in *B. subtilis* that produces SaiR. The wild-type (ORB8820) and *spx* mutant (ORB9050) cells were grown in LB. At OD_{600}=0.3–0.4, cells were treated with NaOCl (final concentration of 2 mM), H_2O_2 (1 mM), or diamide (0.5 mM) for 10 min. RNA purification and cDNA preparation were previously described (Barendt et al., 2013). The fold-induction was shown as averages of biological triplicates with standard deviations after standardized with *rpoB* as described in Experimental procedures.

B. *spxA2*(−247/+268)-*lacZ* was measured in the wild-type strain in the absence (ORB8827) and presence (ORB8820) of the *saiR* gene. The *lacZ* expression was also measured in the strain lacking *B. subtilis spx* in the absence (ORB9049) and presence (ORB9050) of *saiR*.

Table 1

Summary of *spxA1* suppressor mutations

strain	genotype	mutation	effect
ORB8476*	Δ*spxA1 sup1*	BAS3200 (*saiR*) (C95A), *cya* (G2265T)	SaiR (A32E), adenylate cyclase (R755S)
ORB8477	Δ*spxA1 sup2*	BAS3200 (*saiR*) (T83A)	SaiR (I28N)
ORB8478*	Δ*spxA1 sup3*	BAS3200 (*saiR*) (C86T), BAS3859 (C2237T)	SaiR (S29L), pyruvate carboxylase (T746M)
ORB8479	Δ*spxA1 sup4*	BAS3200 (*saiR*) (G179T)	SaiR (G60V)
ORB8480	Δ*spxA1 sup5*	BAS3200 (*saiR*) (G221A)	SaiR (W74 stop)
ORB8492*	Δ*spxA1 sup6*	BAS3200 (*saiR*) (ΔT144)	SaiR (frameshift)
ORB8493	Δ*spxA1 sup7*	BAS3200 (*saiR*) (+T145)	SaiR (H49 stop)
ORB8494	Δ*spxA1 sup8*	BAS3200 (*saiR*) (G32A)	SaiR (S11N)
ORB8495	Δ*spxA1 sup9*	BAS3200 (*saiR*) (ΔACCCA104-108)	SaiR (frameshift)
ORB8496	Δ*spxA1 sup10*	BAS3200 (*saiR*) (ΔT201, ΔA204)	SaiR (L68 stop)
ORB8497	Δ*spxA1 sup11*	BAS3200 (*saiR*) (G181A)	SaiR (G61R)

*Mutations were identified by whole genome sequencing.

Table 2

Genes upregulated by the *saiR* mutation

			Microarray (fold induction)		RT-qPCR (fold induction)	
locus	**gene function**	**gene**	**Δ*saiR*/wt**	**Δ*spxA1*Δ*saiR*/Δ*spxA1***	**Δ*saiR*/wt**	**Δ*spxA1*Δ*saiR*/Δ*spxA1***
BA3456	transcription factor	*spxA2*	15.6	13.1	114.6±33.9	149.7±54.7
BA3455	hypothetical protein		23.5	11.3	110.9±29.8	147.7±47.3
BA3454	hypothetical protein		30.1	22.8	111.8±25.6	132.4±40.5
BA3452	Hypothetical protein		49.2	44.6	N/A	N/A
BA0787	major facilitator family		2.0	13.9	1.6±0.2	3.8±1.4

N/A: not applicable

Values in microarray are medians of triplicates and those in RT-qPCR are averages of triplicates with standard deviations. Locus is shown in *B. anthracis* Ames nomenclature used for microarray. BAS3453 is BAS3200 in *B. anthracis* Ames nomenclature.